

## SHORT PULSE CHARACTERIZATION OF NONLINEARITIES IN POWER ULTRASOUND TRANSDUCERS.

Nicolás Pérez Alvarez, [nicoperez@usp.br](mailto:nicoperez@usp.br)  
Nilson Noris Franceschetti, [nfrances@usp.br](mailto:nfrances@usp.br)  
Flávio Buiochi, [fbuiochi@usp.br](mailto:fbuiochi@usp.br)  
Julio Cezar Adamowski, [jcadamow@usp.br](mailto:jcadamow@usp.br)

University of São Paulo, Department of Mechatronics and Mechanical Systems Engineering  
Av. Prof. Mello Moraes, 2231 São Paulo, Brazil.

**Abstract.** Power ultrasonic transducers are commonly used in industrial applications, such as ultrasonic welding and ultrasonic cleaning. These transducers operate in continuous wave at the resonance frequency, generally around 20 kHz. The driving electronics must follow the resonance frequency in order to obtain maximum efficiency. The resonance frequency changes with the mechanical load, temperature and also with the amplitude of the driving voltage. The dependency of the driving voltage is due to the nonlinear behavior of the piezoceramics. Traditionally, the nonlinear behavior is measured using continuous sinusoidal waves by sweeping the frequency near the resonance of the transducer. Recent works shows improvements to characterize the transducer when using bursts of sinusoidal waves, which minimizes the temperature rising which produces changes in the transducer dynamics. This paper presents a novel technique based on short pulse excitation for the characterization of nonlinear effects of ultrasonic power transducer. The short pulse excitation technique uses a flat spectrum signal near the main resonance frequency. Each component of the input spectrum of the signal is equalized to have the same amplitude and zero phase. The signals are calculated in a computer and sent to an arbitrary function generator, amplified with a power amplifier, and used as an excitation of the transducer using different amplitude levels. It was also implemented a well known sinusoidal burst technique for comparison reason. An experimental comparative analysis of both results shows the differences between the two approaches. It is proposed a simple nonlinear model relating the applied voltage and the displacement of the end surface. The model gives a very good result in the sinusoidal burst technique, and a fair result used for short pulse. The temporal signal is obtained by measuring the displacement at the end surface of the transducer using an optical fiber vibrometer and a digital oscilloscope. The frequency response is obtained by performing the FFT of the signal corresponding to the mechanical displacement. The short pulse technique is very fast when compared to the tone burst analysis and the results are very repetitive. The two techniques are applied in the characterization of two samples of a 20 kHz, 1 kW ultrasonic power transducer.

**Keywords:** Piezoelectric transducer; Power ultrasonics; Non-linear characterization.

### 1. INTRODUCTION

Piezoelectric ceramics have a linear behavior when the applied electric field is below 10 kV/m. Nonlinear effects appear above this electric field (Blackburn and Cain, 2006) which normally happens in high power ultrasonic applications. This work presents theoretical and experimental analysis of a power ultrasonic transducer used in polymer welding applications, shown in Fig. 1. This kind of transducer is formed by a stack of piezoelectric rings sandwiched by two metallic masses, operates as a half wave length resonator, and is known as Langevin-type transducer. The metallic masses are used to give a pre-stress of about 30 MPa to the piezoceramics that support more compression than traction, and to allow better heat exchange. On the other hand, the effect of placing a piezoelectric ceramic stack between end masses is to decrease the operation frequency of the transducer. At one end of the transducer is attached a half wave length mechanical amplifier to increase the displacement amplitude. For this type of transducer, nonlinear effects were originally studied in the frequency domain. Effects such as frequency shift in resonance modes and the "Jumping and Dropping" phenomena were reported by (Umeda et al. 2000). Modified constitutive equations of piezoelectric material can roughly predict nonlinear behavior (Gonnard et al. 1998) (Blackburn and Cain, 2007) (Pérez et al. 1996).

Recent works show the importance to characterize power ultrasonic transducer using sinusoidal burst instead of using continuous wave, because the use of burst minimizes the changes due to temperature increase (Casals et al. 2003) (Blackburn and Cain, 2006). As the continuous wave, the tone burst characterization needs a frequency sweep near the resonance frequency, so this technique becomes time consuming. Another possibility, not reported in the literature, is the use of a wideband pulse containing all the frequencies components near the resonance. The behavior of power ultrasonic transducer operating under high electric field excitation can modeled by nonlinear differential equations, but there are no closed analytical solution for this problem. Considering that it is a transient model, the numerical solution is very high time consuming due to time discretization. This work presents a comparison between the tone burst and the short pulse experimental techniques. The experimental results of these two techniques are used in a parametric nonlinear model that allows the calculation of the time and frequency responses.

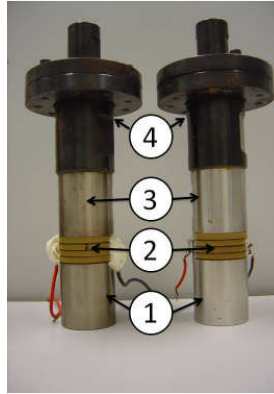


Figure 1. Langevin-type transducer. 1)Tail mass; 2) Piezoelectric disk stack; 3) Head mass; 4) mechanical amplifier

## 2. THEORETICAL MODEL

The theoretical model proposed by (Blackburn and Cain, 2007) relates input voltage with generated current. In the present work this model was modified, relating input voltage  $v_i$  and generated mechanical displacement  $x(t)$ . To reduce the complexity of the model one can suppose that the system is a resonator operating near its resonance frequency. This approximation allows the use of only one parameter to model the nonlinear behavior. The system's response near the resonance is approximated by a mechanical resonator composed by a mass, a spring and a damper, excited by an external force given by the following equation:

$$\ddot{x} + \gamma \dot{x} + \omega_x^2 x = F_{ext} \quad (1)$$

where,  $\gamma$  is the damping coefficient per unit of mass, which models the losses of the system,  $\omega_x$  is the natural frequency and  $F_{ext}$  is the external force per unit of mass. The relation between the linear resonance frequency  $\omega_0$  and the non linear natural frequency  $\omega_x$  is given by the following equation:

$$\omega_x^2 = \omega_0^2 + kX \quad (2)$$

where,  $k$  is a non linear factor and  $X$  is the amplitude of the mechanical displacement. The external force  $F_{ext}$  is proportional to the input voltage  $v_i$ , the proportionality constant  $A$  is used as a parameter in the model.

$$F_{ext} = Av_i = AV_i \cos(\omega \cdot t) \quad (3)$$

The measured time dependent displacement  $x(t)$  when applying a sinusoidal excitation voltage, at a frequency  $\omega$ , is given by:

$$x(t) = X \cdot \cos(\omega \cdot t + \varphi) \quad (4)$$

where  $\varphi$  is the phase angle between the input voltage and the displacement.

Solving Eq. (1) for a monochromatic input one obtain

$$X = \frac{A}{\sqrt{(\omega_x^2 - \omega^2)^2 + \gamma^2 \omega^2}} \quad (5)$$

As  $\omega_x^2$  depends of  $X$ , then the Eq. (5) must be solved iteratively. Figure 2, shows a flowchart of the iterative algorithm to obtain  $X$ .

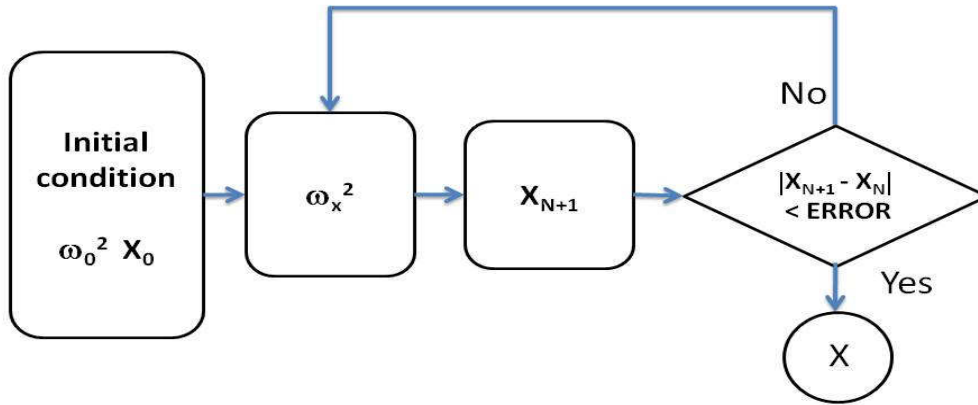


Figure 2. Flowchart of the iterative calculus of  $X$ .

*ERROR* is threshold level to ensure convergence of  $X$ . The parameter set  $[A, \gamma, \omega_0^2, k]$  is adjusted using the `fminsearch` function of Matlab (Nelder-Mead simplex method) where an error function calculates the quadratic difference between the experimental data and the output of the model.

The maximum amplitude of the curve of amplitude versus frequency occurs when:

$$\frac{d((\omega_x^2 - \omega^2)^2 + \gamma^2 \cdot \omega^2)}{d\omega} = 0 \quad (6)$$

The solution of Eq. (6) gives the frequency of maximum amplitude given by:

$$\omega^2 = \omega_x^2 - \frac{\gamma}{2} \quad (7)$$

Considering that  $\gamma$  is very small compared with  $\omega_x^2$ , this term can be neglected and the Eq. (7) becomes:

$$\omega_{max}^2 = \omega_0^2 + k \cdot X_{max} \quad (8)$$

Theoretically, Eq. (8) must be valid for any maximum of all the displacement versus amplitude curves.

### 3. EXPERIMENTAL SETUP AND SIGNAL IMPLEMENTATION

#### 3.1. Signal implementation to sinusoidal burst experiment

The usual practice to characterize ultrasonic power transducers is using sinusoidal signals using a frequency sweep around the main resonance frequency. The experimental procedure is repeated for different levels of the input voltage, obtaining the modulus and the phase of the electromechanical transfer function of the transducer.

The steady state condition of vibration is necessary to obtain the transfer function. Therefore, all the transitory vibrations introduced in the beginning of the burst must be discarded in the measurement. This procedure increases the burst duration. On the other hand, to avoid the temperature rising, the burst should be as short as possible. This means that we have a compromise between a long duration to eliminate the transitory response and a short duration to minimize the temperature rising. The optimal duration is experimentally determinate by measuring the impulse response of the transducer, shown in Fig. 3. It can be seen that the resonance frequency is 19.86 kHz and the duration of the transitory response is less than 50ms which corresponds to 1000 cycles of 20 kHz. It is supposed that the  $X(\omega)$  signal to be analyzed should greater than 10 % of maximum amplitude  $X_{max}$  which corresponds to a bandwidth of about 200 Hz, in this case.

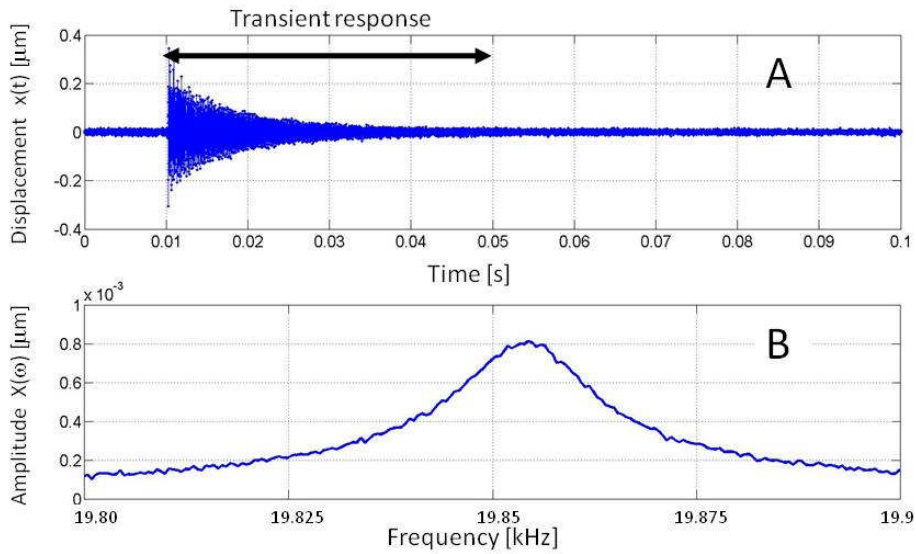


Figure 3. A. Impulse response. B. Spectrum of the impulse response near the main resonance.

Each sinusoidal burst signal is obtained by using 1100 cycles of a sine wave which allows doing the measurement on the last 100 cycles avoiding the transitory region. The period between two consecutive bursts is set to 2 s which means that the transducer is excited less than 3% of time, reducing thermal effects.

### 3.2. Signal implementation to short pulse experiment

A short pulse having the same frequency contents that a set of tone bursts, that is, having a flat frequency spectrum inside the bandwidth of the transducer can be obtained by:

$$v(t) = \sum_{n=1}^N \cos(2 \cdot \pi \cdot f_n \cdot t) \quad (9)$$

where,  $f_n$  is the frequency component,  $N$  is the number of frequencies used to obtain the signal. The number  $N$  is chosen according to the number of steps used in the tone burst experiment.

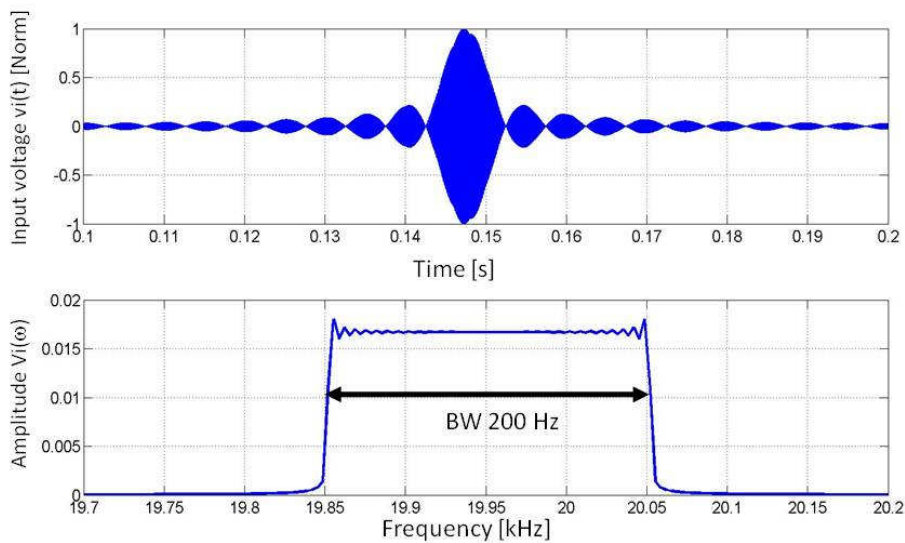


Figure 4. Short pulse BW = 200 Hz. Spectrum amplitude is scaled from the temporal signal.

The spectrum of the signal is approximately flat as shown in Fig. 4. All the frequencies are excited with the same voltage in a single shot when this signal is applied to the transducer. The power of this short pulse is concentrated in a time interval of about 10 ms.

Figure 4 shows that the amplitude of the spectrum relative to the maximum of the temporal signal  $v_i(t)$  is  $17 \times 10^{-3}$ . Table 1 summarizes the characteristics of three different signals used in the experiments.

Table 1. Bandwidth and spectral amplitude of experimental signals.

	<b>BW</b>	<b>Max spectrum</b>
<b>Bandwidth 1</b>	150	$22 \times 10^{-3}$
<b>Bandwidth 2</b>	200	$17 \times 10^{-3}$
<b>Bandwidth 3</b>	300	$11 \times 10^{-3}$

### 3.3. Experimental setup

Figure 5 shows a block diagram of the experimental setup. A personal computer (PC) is used for controlling, data acquisition and signal processing, using the Matlab software. The signals are generated by a programmable arbitrary function generator (Agilent 33250A) and amplified by a power amplifier (Amplifier Research 800A3) using a fix gain of 60 dB. The mechanical displacement is measured by a photonic sensor (MTI 2100) and a digital oscilloscope (Agilent DSO 6052A). The oscilloscope and the function generator are connected to the PC via a GPIB interface (IEEE 488).

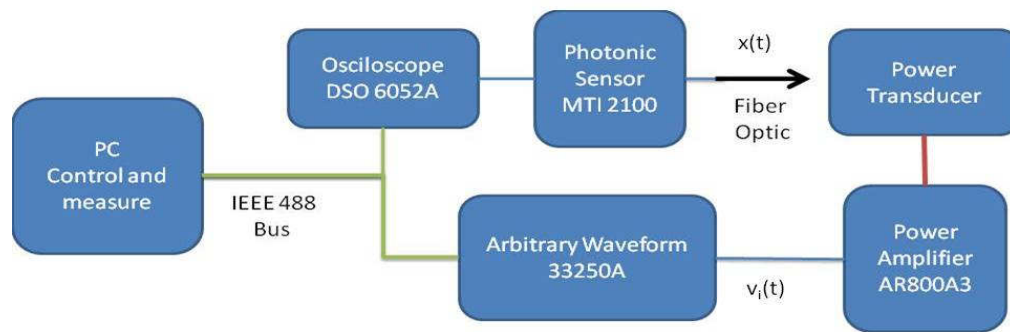


Figure 5. Experimental setup used in both experiments.

It has been experimentally verified, using a resistive electrical load, that the maximum input voltage must be under 400 mV to avoid the nonlinear behavior of the power amplifier. Considering that the amplifier gain is 60 dB, the electric field applied to the piezoceramic is obtained using the relationship: 1 mV input in the power amplifier corresponds to 200 V/m applied to the piezoceramic.

## 4. SINUSOIDAL BURST CHARACTERIZATION

The results presented in this section are measured over 200 frequency points using the bursts described in section 3.1. The interval between two adjacent frequencies is 1 Hz covering a bandwidth of 200 Hz. The measurements are performed using the following input voltages: 1mV, 2mV, 4mV, 8mV, 16mV, and 64mV.

Figure 6 shows the results of the sinusoidal burst characterization. The results are fitted using the theoretical model introduced in section 2. It can be observed that the model reproduces the results closely.

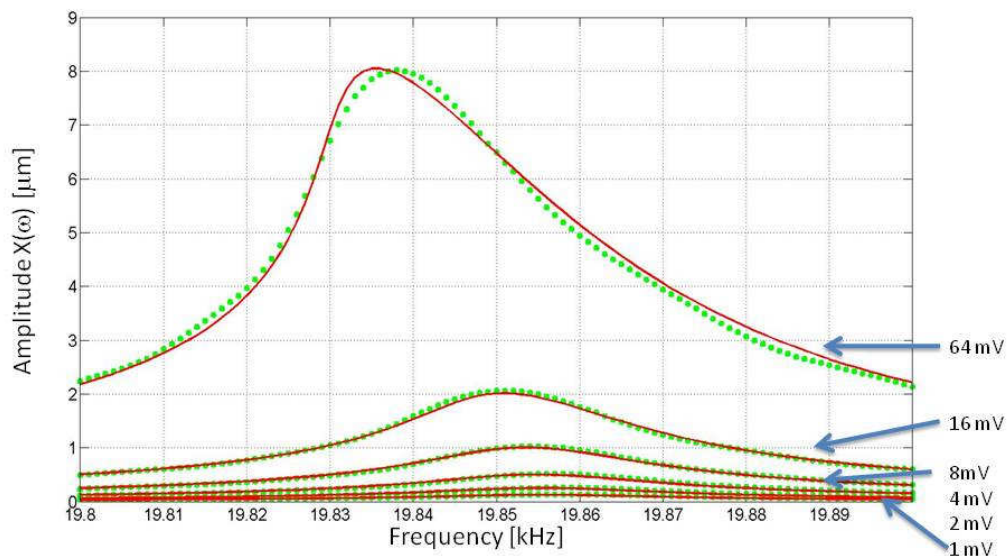


Figure 6. Results using sinusoidal bursts. Dotted line (experimental). Model fit (solid line).

The following nonlinear effects are observed in the transducer response: (a) the resonance frequency decreases from 19.856 kHz to 19.836 kHz when the input voltage increases from 1 mV to 64 mV; (b) the mechanical quality factor decreases and the curves lose symmetry when the amplitude is increased.

To validate the theoretical model proposed in section 2, represented by Eq. (8), the experimental values of  $\omega_{max}^2$  are plotted against the corresponding amplitude of oscillation  $X_{max}$ . Figure 7, shows the experimental results and a linear approximation. This result shows a good agreement between experimental and the prediction of the proposed model.

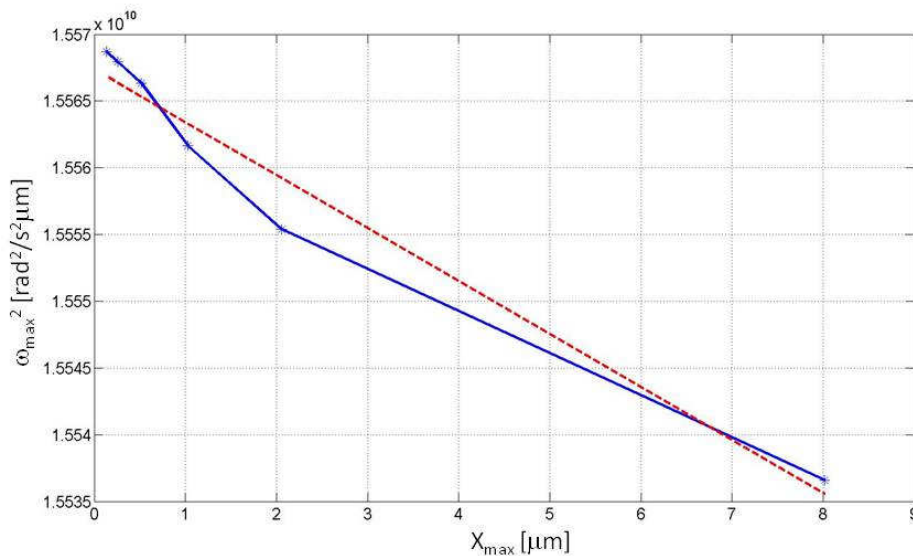


Figure 7. Relationship between  $\omega^2$  and the amplitude  $X$  for the maximum of each frequency response curve. Experimental data, solid line “\*”. Least squares fit, dashed line.

## 5. SHORT PULSE CHARACTERIZATION

The first step for the short pulse characterization is the signal construction following the procedure detailed in section 3.2. The selected set for the maximum input voltage  $v_i(t)$  is [50mV, 100mV, 150mV, 200mV, 250mV, 300mV, 350mV]. An input level lower than 50 mV produces a small response that is affected by the noise; on the other hand, the maximum input voltage used is 350 mV not to exceed the limit of the electronic linear behavior.

Figure 8 shows the result of applying four different amplitude levels. The temporal response remains large for a longer time than the input signal duration because the transitory response of the transducer is about 50 ms.

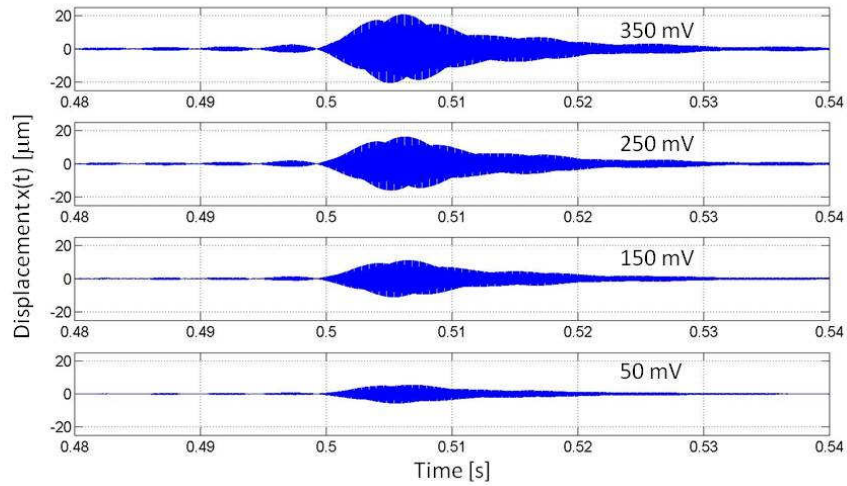


Figure 8. Short pulse signal temporal response for input values [50 mV, ..., 350 mV] correspond to the maximum input voltage  $v_i(t)$  shown in Fig.4.

To obtain a spectrum that can be compared with the result set obtained in the burst mode, the total signal duration  $T$  and the sampling frequency  $F_{sample}$  must be selected. The number of samples to be acquired  $N_{sample}$  is the product of these last two values.

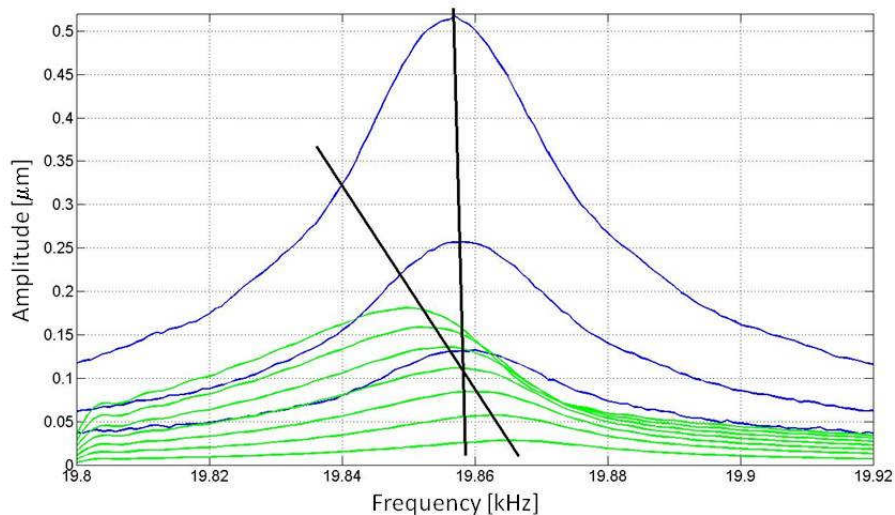


Figure 9. Short pulse excitation results (green) for input range [50mV, 100mV, 150mV, 200mV, 250mV, 300mV, 350mV]. Burst mode results (blue), using range [1mV, 2mV, 4mV].

The  $F_{sample}$  was selected as 100 kHz, which allows reproducing the system response up to 50 kHz, more than two times greater than the main resonance frequency. The total duration  $T$  was selected to  $T = 1$  s, reproducing the frequency interval of 1 Hz used in sinusoidal burst experiments.

$$df = \frac{F_{sample}}{N_{sample} - 1} = \frac{1}{T} = 1 \text{ Hz} \quad (10)$$

To analyze the results, the signal spectrum is calculated using the FFT. In Fig.9, these spectrums are plotted for a set of input voltage amplitudes from 50 mV to 350 mV in steps of 50 mV (green curves). As a reference, the three blue curves of sinusoidal analysis and two straight lines to highlight the evolution of the resonance peak for each case were included. There are two main characteristics: the pulse signal frequency shift is high when compared to the burst signal and the curve shapes differ in both experiments.

To obtain a quantitative result for this pulsed signal, Eq. (8) is used. The  $\omega^2$  and the  $X$  values for the maximum of each curve are adjusted by a straight line, as in Fig.7. Thus, the natural frequency  $f_0$  and the nonlinear coefficient  $k$  are obtained. The calculus of  $k$  using Eq. (8) is faster than the full model adjustment and gives similar results.

Figure 9, shows the result of the applied pulsed signals summarized in Tab. 1. The values of  $k$  (slope of the straight line) are much repetitive than  $f_0$ . Numerical values for the parameters are given in next section.

Although the amplitudes  $X$  of the spectrum are small (less than  $0.3\mu\text{m}$ ), the temporal displacement  $x(t)$  amplitudes are in the order of  $10\mu\text{m}$ . This means that the nonlinear behavior can be greater than the expected in the sinusoidal model such behavior comes from an  $x^2$  coefficient, instead of a  $X(\omega) \cdot x(t)$  coefficient, as used in the model.

Also, the shape change can be explained by this effect. The frequency components under the resonance frequency, have higher amplitudes than predicted by the sinusoidal model. Thus, there is a need to obtain a better model to predict the results in the pulse regimen, although in a first approximation the nonlinear coefficient  $k$  takes into account the factor introduced by the instantaneous value of  $x(t)$ .

Responses to the different bandwidth signals are shown in Fig.9. A signal whit a narrow spectrum produces greater output amplitude.

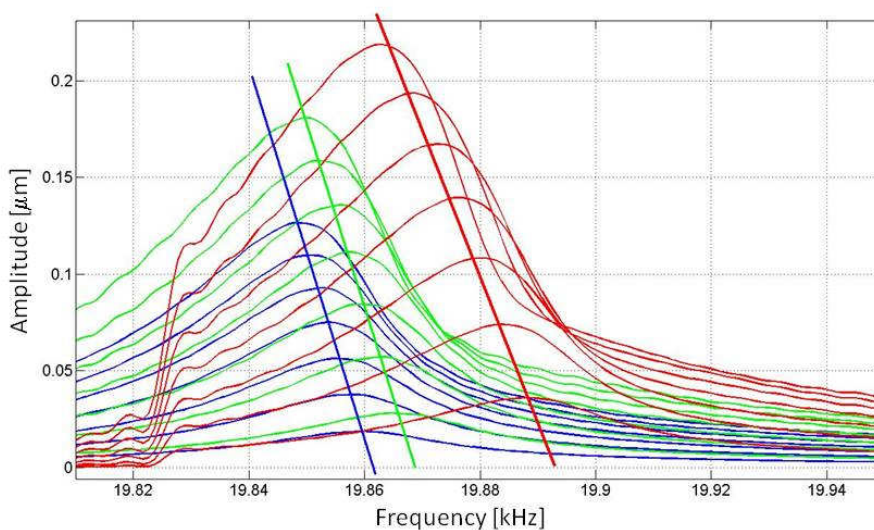


Figure 10. Results for three different bandwidth signals. Red - 150Hz, Green - 200Hz, Blue - 300Hz.

## 6. CONCLUSIONS

An experimental characterization of Langevin transducer nonlinear behavior was done by using sinusoidal bursts and short pulse signals. As a first step, a methodology to construct the signals was developed. The frequency range used was the same for both cases, in order to compare the results.

For quantitative comparisons, a simple input-output model for the transducer electromechanical transfer function was proposed. It is an adaptation of the electrical model proposed by Blackburn and Cain (2006). The nonlinear effects were introduced by using only one parameter, the coefficient  $k$ .

The model was validated for the experimental data using Eq. (8) and the results reproduced the system response to a sinusoidal input for a range much larger than the used in the pulse experiment. For the case of sinusoidal inputs, the model allows a good prediction of the system behavior.

In the case of short pulse signals, the qualitative behavior was the same. But the resonance frequency decreases when the input voltage is increased in a faster way than for the burst mode case. However, the curve shape is different from those obtained in the burst mode experiments.

Table 2 summarizes the results for two transducers, both constructed to work at 20 kHz, and four different signals: sinusoidal burst, 150-Hz-bandwidth short pulse, 200-Hz-bandwidth short pulse, and 300-Hz-bandwidth short pulse.

The implemented model should be used cautiously. Because the coefficients  $k$ , introduced in Eq. (8), have shown to vary 50 times faster in the case of pulsed signals.

The differences between the sinusoidal model and the short pulse experiment can be explained by the response dependence on the instantaneous oscillation  $x(t)$ . In a future work, the theoretical model should be adapted to precisely reproduce the results for the pulsed mode.

Table 2. Experimental Parameters

	Sinusoidal Burst				Pulse [BW 150 Hz]		Pulse [BW 200 Hz]		Pulse [BW 300 Hz]	
	$A$ $\mu\text{m}/\text{mV}$	$\gamma$ $\mu\text{m}/\text{s}$	$f_0$ Hz	$K$ $\text{rad}^2/\text{s}^2 \mu\text{m}$	$f_0$ Hz	$k$ $\text{rad}^2/\text{s}^2 \mu\text{m}$	$f_0$ Hz	$K$ $\text{rad}^2/\text{s}^2 \mu\text{m}$	$f_0$ Hz	$K$ $\text{rad}^2/\text{s}^2 \mu\text{m}$
<b>Transducer A</b>	$2.8 \times 10^6$	178	19856	$-3.98 \times 10^6$	19894	$-207 \times 10^6$	19868	$-153 \times 10^6$	19861	$-152 \times 10^6$
<b>Transducer B</b>	$4.94 \times 10^6$	302	20275	$-2.05 \times 10^6$	20282	$-115 \times 10^6$	20274	$99 \times 10^6$	20273	$85 \times 10^6$

## 7. ACKNOWLEDGEMENTS

We would like to thank the State of São Paulo research agency FAPESP for financial support.

## 8. REFERENCES

- Arafa, M. and Baz, A., 2004, "On the Nonlinear Behavior of Piezoelectric Actuators" Journal of Vibration and Control, Vol. 10, pp 387-398.
- Blackburn, J. and Cain, M., 2006, "Nonlinear piezoelectric resonance: A theoretically rigorous approach to constant I-V measurements." Journal of Applied Physics Vol.100, 114101.
- Blackburn, J. and Cain, M., 2007, "Non-linear piezoelectric resonance analysis using burst mode: a rigorous solution" J. Phys. D: Appl. Phys. Vol. 40, pp. 227–233.
- Casals, J., Albareda, A., Pérez, R., García, J., Minguella, E. and Montero de Espinosa, F., 2003, "Nonlinear characterization with burst excitation of 1–3 piezocomposite transducers." Ultrasonics 41. pp 307–311.
- Gonnard, P., Perrin, V., Briot, R., Guyomar, D. and Albareda, A., 1998, "Characterization of the piezoelectric ceramic mechanical nonlinear behavior." Proceedings of the IEEE International Symposium ISAF 1998, pp. 353-356.
- Perez, R., Albareda, A., Minguella, E. and Villar, J.L., 1996, "Electrical model for a nonlinear piezoelectric transducer." Proceedings of the IEEE Applications of Ferroelectrics, Vol. 2, pp 955-958.
- Pérez, N., Franceschetti, N. and Adamowski, J.C., 2009, "Effects of Nonlinearities in Power Ultrasonic Transducers Using Time Reversal Focalization." To be appear in 2009 ICU Proceedings.
- Umeda, M., Nakamura, K., Takahashi, S. and Ueha, S., 2000, "An Analysis of Jumping and Dropping Phenomena of Piezoelectric Transducers using the Electrical Equivalent Circuit Constants at High Vibration Amplitude Levels." Japan Journal of Applied Physics, Vol.39; N° 9B, pp.5623-5628.

## 9. RESPONSIBILITY NOTICE

The authors are the only responsible for the printed material included in this paper.